



NLR-TP-2005-205

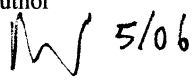
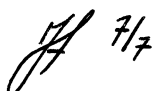
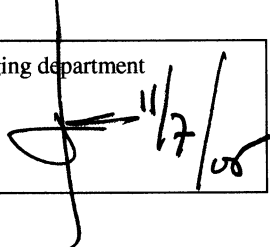
Corrosion-induced cracking of model train zinc-aluminium die castings

R.J.H. Wanhill and T. Hattenberg

This report may be cited on condition that full credit is given to NLR and the authors.

Customer: National Aerospace Laboratory NLR
Working Plan number: AV.1.M
Owner: National Aerospace Laboratory NLR
Division: Aerospace Vehicles
Distribution: Unlimited
Classification title: Unclassified
May 2005

Approved by:

Author	Reviewer	Managing department
 5/06	 7/7	 11/7/06



Content

1	Introduction	3
2	Zinc-aluminium die castings	4
3	Corrosion-induced cracking	6
4	Discussion: corrosion initiation, progression, and a possible countermeasure	8
5	Conclusions	10
6	References	10

9 Figures

Corrosion-induced Cracking of Model Train Zinc-Aluminium Die Castings

R.J.H. Wanhill and T. Hattenberg

National Aerospace Laboratory NLR, Amsterdam, The Netherlands

Abstract

Corrosion-induced cracking of model train zinc-aluminium die castings is described and explained from previous knowledge and a new investigation. The corrosion results from impurities in the metal, and requires the presence of moisture. Cracking proceeds inwards from external surfaces, mainly along the β phase boundaries but also through the $(\alpha'+\beta)$ eutectic. Corrosion product build-up in the cracks causes swelling of the castings. A possible countermeasure, the application of a parylene coating, is suggested for suspect or slightly damaged items.

Keywords: zinc alloys, castings, corrosion, microstructure, coatings

1 Introduction

Some model train die castings made from zinc-aluminium alloys and produced in the first decade after World War II have shown susceptibility to corrosion-induced cracking. The susceptibility varies, but in severe cases leads to disintegration of the model, see figure 1.

Many models of this vintage are valuable collectors' items. It is important to preserve them, provided they are judged to be undamaged or only slightly damaged. However, the corrosion is generally considered unstoppable.

Here we discuss the problem of corrosion-induced cracking in detail, and then suggest a possible countermeasure. The problem needs thorough discussion because information available to the non-specialist, notably via the internet, often contains errors.

2 Zinc-aluminium die castings

Alloy development

The origin of zinc die castings is a bit uncertain. Bierbaum (1923) mentions zinc-copper-aluminium die castings made as early as 1896, while Goodway (1985) and Gross (2003) state that the first commercial alloy was produced around 1907. By the early 1920s it was recognised that alloys based on the zinc-aluminium binary system were easy to cast and had good mechanical properties. At the same time, it became clear that the control of impurity elements was vital: small amounts of lead, cadmium and tin resulted in corrosion-induced cracking and swelling of the castings (Brauer and Pierce 1923).

Some alleviation of the corrosion problem was obtained by additions of copper to the impure binary alloys (Brauer and Pierce 1923), but its elimination was achieved only by the use of special high purity zinc (99.99%) and further additions of small amounts of magnesium (Goodway 1985; Gross 2003). These developments took place during 1926-1929, leading to introduction of the ZAMAK¹ series of alloys, several of which are still in use today, see table 1. This table also includes the ZA alloys, developed and introduced in the 1960s and 1970s (Apelian *et al.* 1981; Gross 2003). Note that all the alloys have specified ranges and values for the alloying elements, and very low impurity limits for lead, cadmium and tin.

Table 1 Chemical compositions of current zinc die casting alloys (weight %)

Element	ZAMAK 3	ZAMAK 5	ZAMAK 7	ZA-8	ZA-12	ZA-27
aluminium	3.5-4.3	3.5-4.3	3.5-4.3	8.0-8.8	10.5-11.5	25.0-28.0
magnesium	0.02-0.05	0.03-0.08	0.005-0.02	0.015-0.03	0.015-0.03	0.015-0.02
copper	0.25	0.75-1.25	0.25	0.8-1.3	0.5-1.2	2.0-2.5
iron	0.10	0.10	0.075	0.075	0.075	0.075
nickel	-	-	0.005-0.02	-	-	-
lead	0.005	0.005	0.003	0.006	0.006	0.006
cadmium	0.004	0.004	0.002	0.006	0.006	0.006
tin	0.003	0.003	0.001	0.003	0.003	0.003

¹ ZAMAK : trademark of the New Jersey Zinc Company



Basic metallurgy

As table 1 shows, current zinc die castings are basically binary alloys of zinc and aluminium. The starting point for understanding the metallurgy of these alloys is the zinc-aluminium equilibrium phase diagram, figure 2. The main features of this diagram are:

- Liquid alloy undergoes a eutectic transformation at the composition 94 wt.% Zn-6 wt. % Al and at 381°C. The transformation products are the α' phase (83.1 wt. % Zn) and β phase (98.8 wt. % Zn).
- Below 277°C the α' phase is unstable and undergoes a eutectoid transformation. The transformation products are α phase (32.4 wt. % Zn) and β phase (99.3 wt. % Zn).
- The solid solubility of aluminium in β decreases from 1 wt. % at the eutectic temperature to almost zero at room temperature. The solid solubility of zinc in α' decreases from 83.1 wt. % at the eutectic temperature to 77.7 wt. % just before the eutectoid transformation. The solid solubility of zinc in α decreases from 32.4 wt. % at the eutectoid temperature to about 1 wt. % at room temperature.

Copper and magnesium additions to the binary alloys retard the eutectoid transformation, but the amounts present in commercial alloys, table 1, would not be expected to prevent it, see Apelian *et al.* (1981). Another point to be made about the equilibrium phase diagram is the aluminium contents of the commercial alloys. The ZAMAK alloys contain less than 6 wt. % Al, and are referred to as *hypoeutectic* alloys. The ZA alloys contain more than 6 wt. %, and are therefore referred to as *hypereutectic* alloys.

In the remainder of this section we shall consider only hypoeutectic alloys, since these were used for vintage model trains.

Solidification of hypoeutectic alloys

Figure 3 shows the zinc-rich part of the zinc-aluminium equilibrium phase diagram and the cooling trajectory for a hypoeutectic alloy having bulk composition X. As the alloy cools in the liquid phase region, it eventually reaches the liquid/(β +liquid) phase boundary line between the eutectic point and the melting point of pure zinc (419.58°C). Further cooling results in solidification of zinc-rich crystals (β phase dendrites²) until

²Dendrite crystals are so-called because they branch more or less like trees.



the eutectic temperature is reached. Then the remaining liquid solidifies interdendritically as a eutectic mixture of α' and β .

Continued cooling *under nominally equilibrium* conditions would cause the following solid state compositional changes in the primary β and the eutectic α' and β :

- The aluminium content of the β phase decreases slightly, following the $(\alpha'+\beta)/\beta$ phase boundary line till 277°C, and then the $(\alpha+\beta)/\beta$ phase boundary line. The result is precipitation of minute particles of α within the β phase.
- The zinc content of the α' phase decreases, following the $\alpha'/(\alpha'+\beta)$ phase boundary line between the eutectic (83.1 wt. % Zn, 16.9 wt. % Al) and eutectoid (77.7 wt. % Zn, 22.3 wt. % Al) transformation temperatures.
- At the eutectoid temperature the α' decomposes into α and β , as mentioned above. With further cooling the zinc content of the α phase decreases from 32.4 wt. % to about 1 wt. %, following the $\alpha/(\alpha+\beta)$ phase boundary line shown in figure 2.

However, die casting results in fast cooling of the metal and non-equilibrium conditions, notably for solid state reactions, which are slow compared to those in liquids. Thus in practice a die cast hypoeutectic alloy should retain a microstructure of β phase crystals, surrounded by a eutectic mixture of α' and β (Apelian *et al.* 1981; Mongeon and Barnhurst 1985).

Figure 4 gives examples of the microstructures of the wheel and block shown in figures 1b and 1c. The wheel's microstructure consists of fine β crystals surrounded by fine eutectic, indicating rapid solidification. The block's microstructure is coarser, owing to less rapid solidification, and there is relatively more eutectic, whose lamellar structure is evident. Also, at this magnification it is just possible to observe α particles within the β crystals: see also figure 8b.

3 Corrosion-induced cracking

Background information

Brauer and Pierce (1923) investigated the corrosion-induced cracking of zinc alloy cast bars in some detail. Their results and conclusions may be summarised as follows:



- Corrosion proceeds from the surface inwards, is intercrystalline, and attacks the β phase.
- Moisture is *essential* to the occurrence of corrosion, which is also accelerated by higher temperatures.
- Corrosion severity, as measured by swelling of the castings, depends on alloy impurities, or other metals deliberately added, and also the alloy grain or crystal size. In particular, the impurities lead, cadmium and tin result in very severe corrosion. A finer crystal size, owing to more rapid solidification, causes a general increase in corrosion. Brauer and Pierce suggested that the detrimental effect of a finer crystal size is due to the greater number of intercrystalline boundaries where corrosion can occur.

Evans (1923, 1925) provided an electrochemical explanation for the effect of impurities on zinc corrosion. Evans observed that the cathodic reaction (evolution of hydrogen gas) during zinc corrosion is facilitated by intercrystalline impurities and also by impurities dissolved out of solid solution and redeposited as a sponge.

Evans' explanation fits firstly with the fact that lead and tin are virtually insoluble in solid zinc and solid aluminium (Baker *et al.* 1992) and have melting points lower than zinc and the eutectic. Lead and tin therefore solidify at the $\beta/(\alpha'+\beta)$ boundaries, i.e. they are intercrystalline impurities *a priori*. Secondly, small amounts of cadmium (up to about 2.5 wt. %) will be in solid solution in the β phase (Mongeon and Barnhurst 1985; Baker *et al.* 1992). Initial corrosion will attack the β phase via its crystal boundaries and dissolve out the cadmium, which presumably redeposits as a sponge and then acts as an intercrystalline impurity *a posteriori*.³

Model locomotive wheel and block

Figure 5 gives metallographic overviews of the cracking in the wheel and block. The cracks began from the external surfaces. Note the porosity owing to gas entrapment during casting, especially throughout the wheel. This indicates non-optimum casting practice, although the pores would not have affected using the components.

³ Gross (2003) incorrectly stated that cadmium has extremely low solid solubility in zinc, and that this, coupled with its lower melting point, causes cadmium to solidify in grain (i.e. crystal) boundaries.

Details of the cracking were obtained with an SEM + EDX combination.⁴ The results are summarised in table 2 and illustrated in figures 6-9. These results are additional to those of Brauer and Pierce (1923), since the SEM + EDX enabled more details. Thus the cracking is not only along the β boundaries, but can also pass through the eutectic. The important role of lead particles in directing the crack paths is also clear, at least for the block. Finally, the swelling that accompanies corrosion is due to corrosion product build-up in the cracks. The corrosion product is poorly adherent, since it is missing in the widely opened cracks at the external surfaces, e.g. figures 1b and 1c.

Table 2 Metallographic details of cracking in the wheel and block

<ul style="list-style-type: none">● wheel<ul style="list-style-type: none">- cracks mainly along β boundaries and also through the eutectic- cracks largely or wholly filled with corrosion products- minute lead particles on porosity cavity walls● block<ul style="list-style-type: none">- cracks favour β boundaries but also run extensively through the eutectic- cracks largely or wholly filled with corrosion products- lead particles in matrix, along cracks and on porosity cavity walls
--

4 Discussion: corrosion initiation, progression, and a possible countermeasure

Corrosion initiation and progression

From the literature (Brauer and Pierce 1923; Evans 1923,1925) and the present work we may conclude the following:

- (1) Corrosion of zinc die castings is an electrochemical process facilitated - or indeed caused - by small amounts of impurities in the metal, notably lead, cadmium and tin.
- (2) Because the corrosion is electrochemical, it requires moisture to initiate and progress, which is why it proceeds inwards from external surfaces. The electrochemical nature also explains why higher temperatures accelerate the corrosion.

⁴ Scanning Electron Metallography (SEM) + Energy Dispersive analysis of X-rays (EDX)



- (3) Corrosion is characterised by cracking, mainly along the β phase (zinc-rich) crystal boundaries, but also through the $(\alpha'+\beta)$ eutectic.
- (4) The swelling of the castings that accompanies corrosion is due to corrosion product build-up in the cracks.

Bearing these conclusions in mind, especially conclusion (2), we can now discuss a possible countermeasure for vintage model train die castings that are judged to be undamaged or only slightly damaged.

A possible countermeasure

It is over 50 years since some model train die castings were made from zinc-aluminium alloys containing too-high amounts of one or more of the impurity elements lead, cadmium and tin. Nevertheless, the problem of corrosion-induced cracking and its progression is still very much a concern to collectors. If corrosion-induced cracking is present it is generally considered unstoppable. However, recent developments in coating technology (Wood 2000) suggest a possible countermeasure, namely the application of a colourless polymer coating with the generic name "Parylene".

Parylene coatings are deposited by vapour condensation in a low-pressure (partial vacuum) environment at ambient temperatures. This method is advertised to provide pinhole-free uniform coatings with controllable thicknesses as little as 0.2 μm and up to 75 μm . The coatings resist solvents, acids and bases, have low permeability to moisture, and are stable up to 200°C (www.vp-scientific.com/parylene_properties.htm 2004).

In addition, parylene coatings would appear to offer an important advantage for any items that could, or actually do, contain cracks. This is their application in a low-pressure environment, which means that much of the moisture entrapped in any cracks or crevices is likely to be pumped away before coating. Ambient temperature application is also advantageous, since thermal stressing of the items is avoided.

Parylene coating installations are too expensive and specialised for private purchase and use. Coating would have to be done by specialist firms. The costs involved could be mitigated by coating items in batches, since the deposition chambers are large, with capacities up to about 500 litres.



A final point to consider is the possibility of a validation exercise. This would have to be negotiated with a parylene coating firm. The validation would require samples from corrosion-damaged items of little or no remaining value, and cover the following main points:

- Accelerated corrosion testing of coated and uncoated samples: air at 95°C and 100% relative humidity for 10 days under conditions permitting condensation of hot water on the metal (Corbett and Saldanha 1987).
- Sample appearances before and after coating. The coatings should be virtually invisible over a reasonable range of thicknesses.

5 Conclusions

Corrosion-induced cracking of model train zinc-aluminium die castings is caused by small amounts of impurities in the metal, notably lead, cadmium and tin. The corrosion requires moisture to initiate and progress, and is accelerated by higher temperatures. A possible countermeasure is to apply parylene coatings to suspect or slightly damaged items. This would have to be done by specialist firms.

6 References

Apelian, D., Paliwal, M., Herrschaft, D.C., 1981, Casting with Zinc Alloys, *Journal of Metals*, Vol. 33, November 1981, pp.12-20.

Baker, H., *et al.* (Editors), 1992, *ASM Handbook Volume 3, Alloy Phase Diagrams*, ASM International, Materials Park, Ohio, USA, pp. 2·42, 2·49, 2·52, 2·56, 2·131, 2·337, 2·372.

Bierbaum, C.H., 1923, Discussion in: *Transactions of the American Institute of Mining and Metallurgical Engineers*, Vol. 68, p. 828.

Brauer, H.E., Pierce, W.M., 1923, The Effect of Impurities on the Oxidation and Swelling of Zinc Aluminum Alloys, *Transactions of the American Institute of Mining and Metallurgical Engineers*, Vol. 68, pp.796-826.



Corbett, R.A., Saldanha, B.J., 1987, Evaluation of intergranular corrosion, *Metals Handbook Ninth Edition, Volume 13, Corrosion*, American Society for Metals, Metals Park, Ohio, USA, pp. 239-241.

Evans, U.R., 1923, The Electrochemical Character of Corrosion, *Journal of the Institute of Metals*, Vol. 30, pp. 239-282.

Evans, U.R., 1925, Surface Abrasion as a Potential Cause of Localized Corrosion, *Journal of the Institute of Metals*, Vol. 33, pp. 27-43.

Goodway, M., 1985, Disintegration of Zinc Die-Castings, *Journal of the Historical Metallurgy Society*, Vol. 19, No. 1, pp. 37-38.

Gross, D.K., 2003, Zinc Die Castings – The Importance of Alloy Chemistry, *Die Casting Engineer*, Vol. 47, No. 2, pp. 30-31.

Mongeon, L., Barnhurst, R.J., 1985, Zinc and Zinc Alloys, *Metals Handbook Ninth Edition, Volume 9, Metallography and Microstructures*, American Society for Metals, Metals Park, Ohio, USA, pp. 488-496.

Wood, R., 2000, To Protect and Preserve, *Materials World*, Vol. 8, No. 6, pp. 30-32.

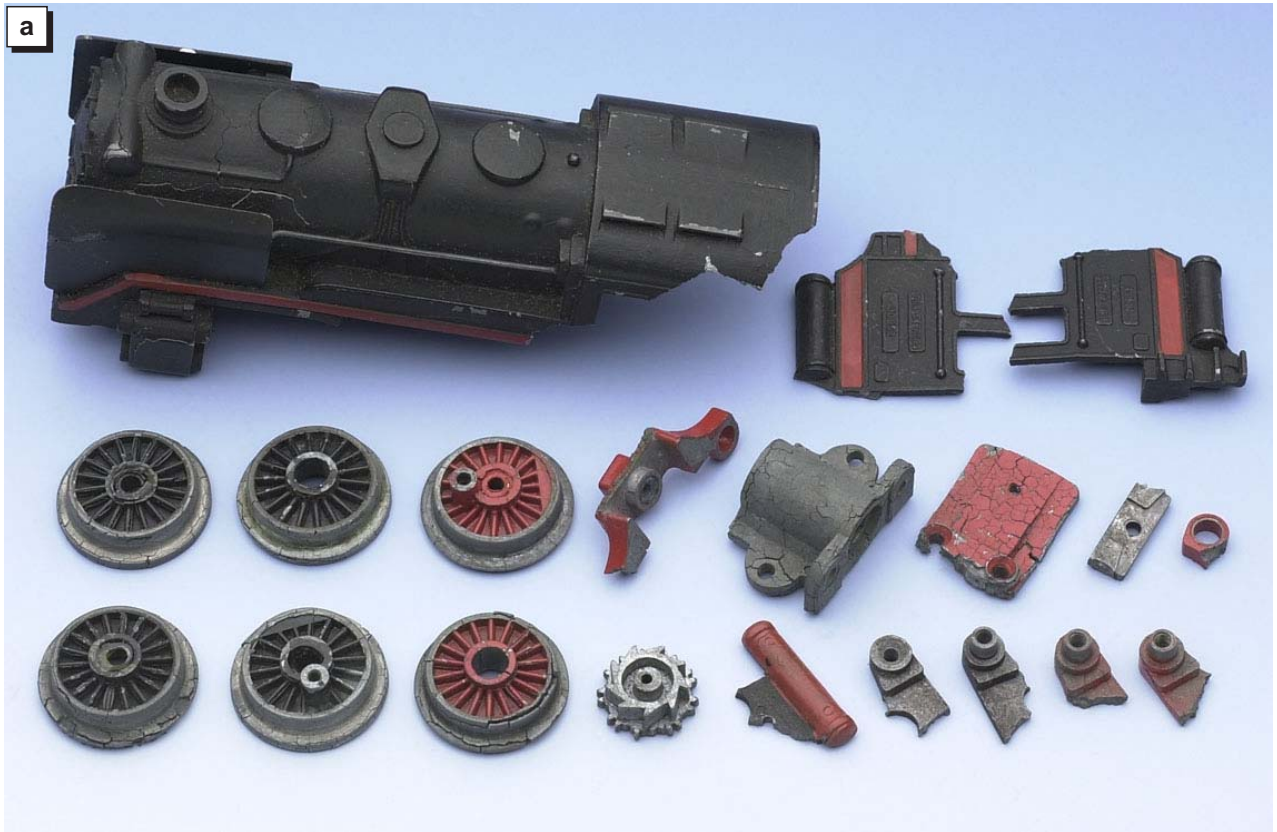


Fig. 1 Severe corrosion-induced cracking in a zinc-aluminium die cast model locomotive, vintage 1946-1947. The details in figures 1b and 1c show part of a wheel and a block fitting

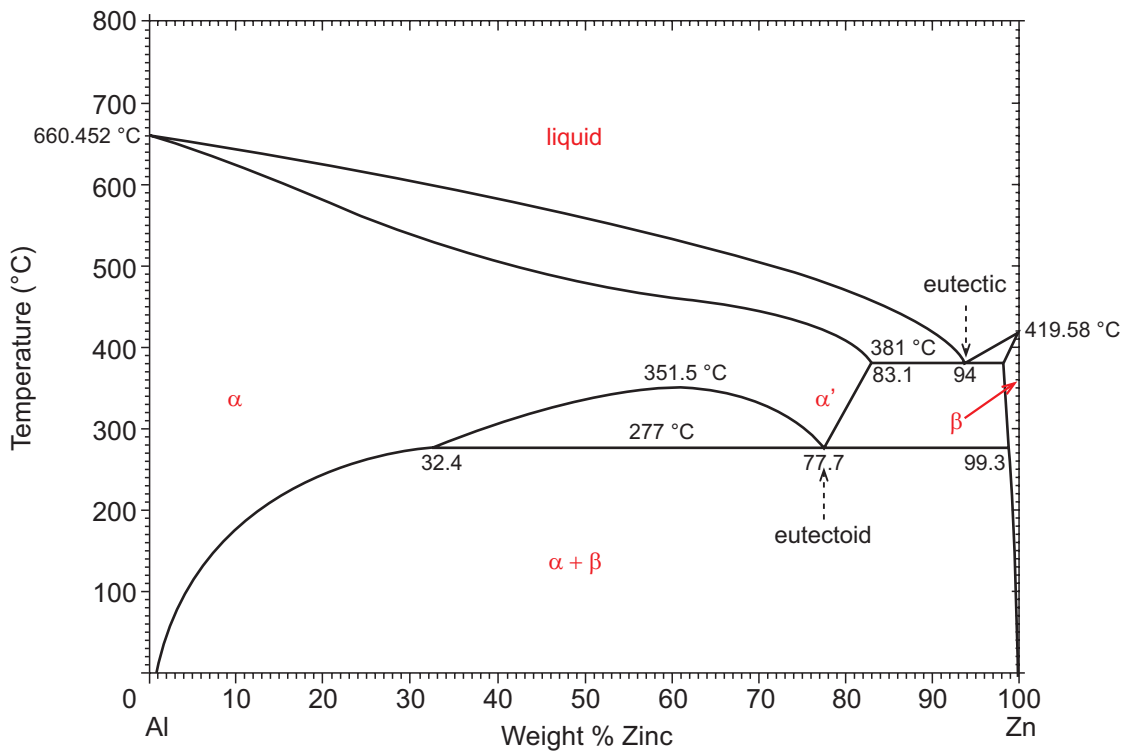


Fig. 2 Zinc-aluminium equilibrium phase diagram: permission ASM International, see Baker et al. (1992), p. 2-56

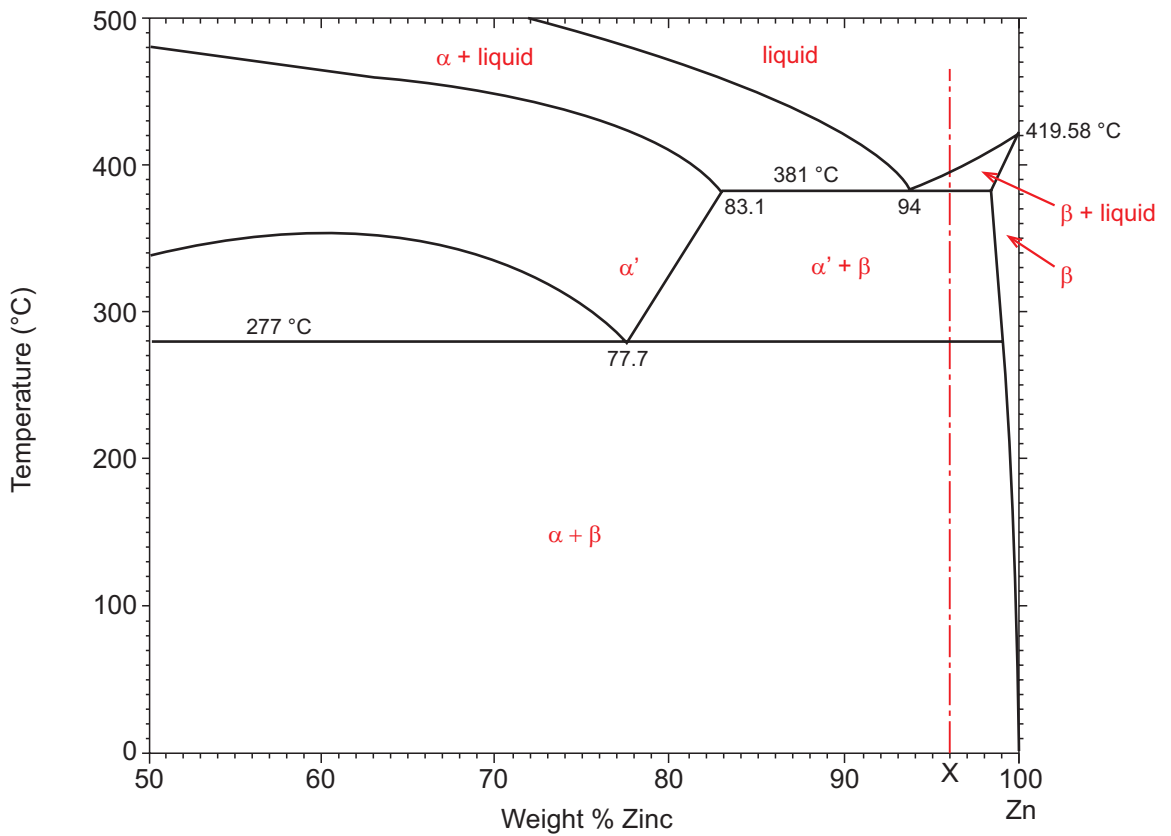


Fig. 3 Zinc-rich part of the zinc-aluminium equilibrium phase diagram and the cooling path of a hypoeutectic alloy having bulk composition X

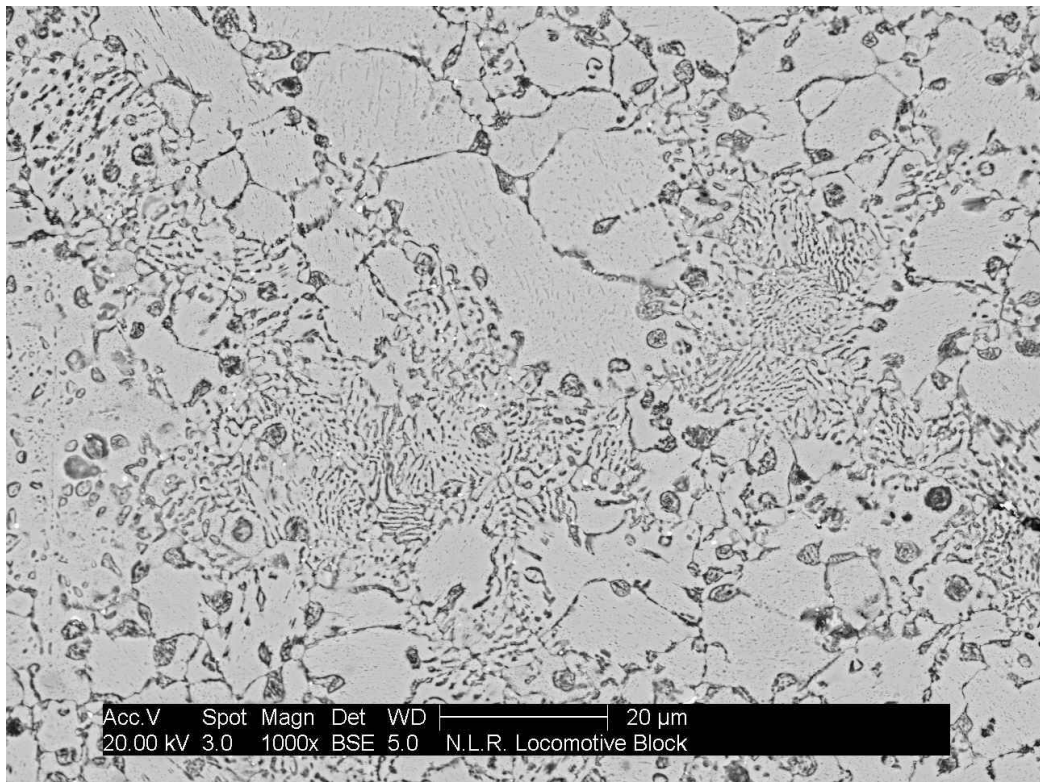
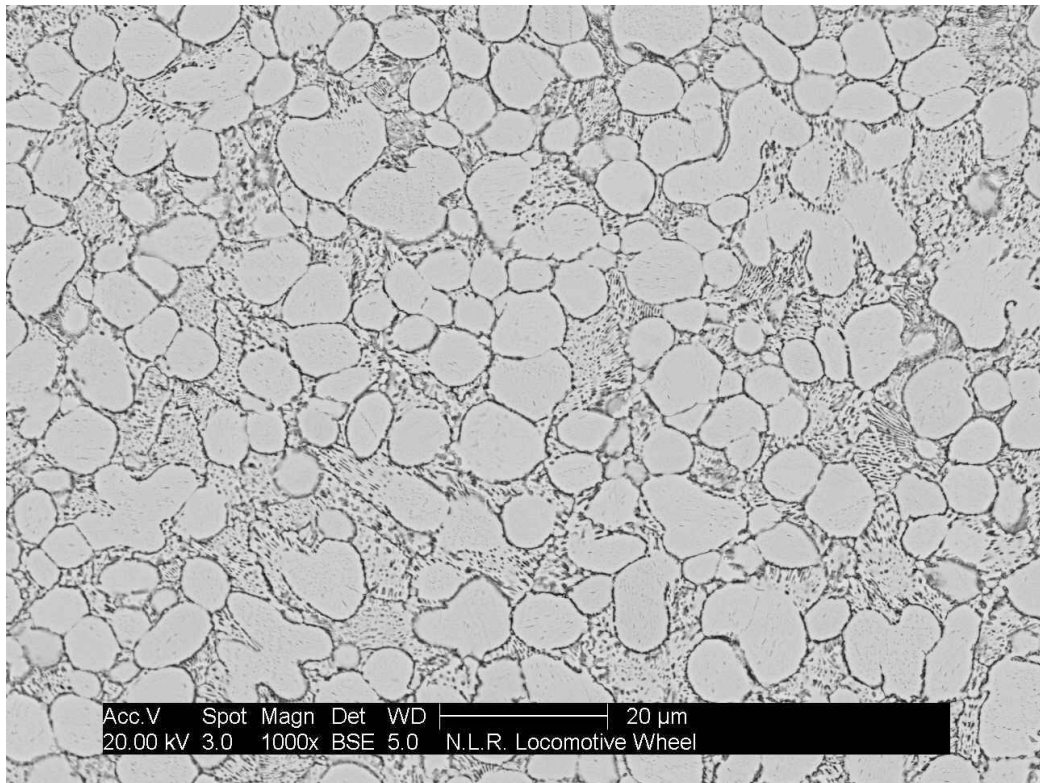


Fig. 4 Microstructures of the wheel and block shown in figures 1b and 1c:
SEM metallographs, backscattered electron (BSE) imaging

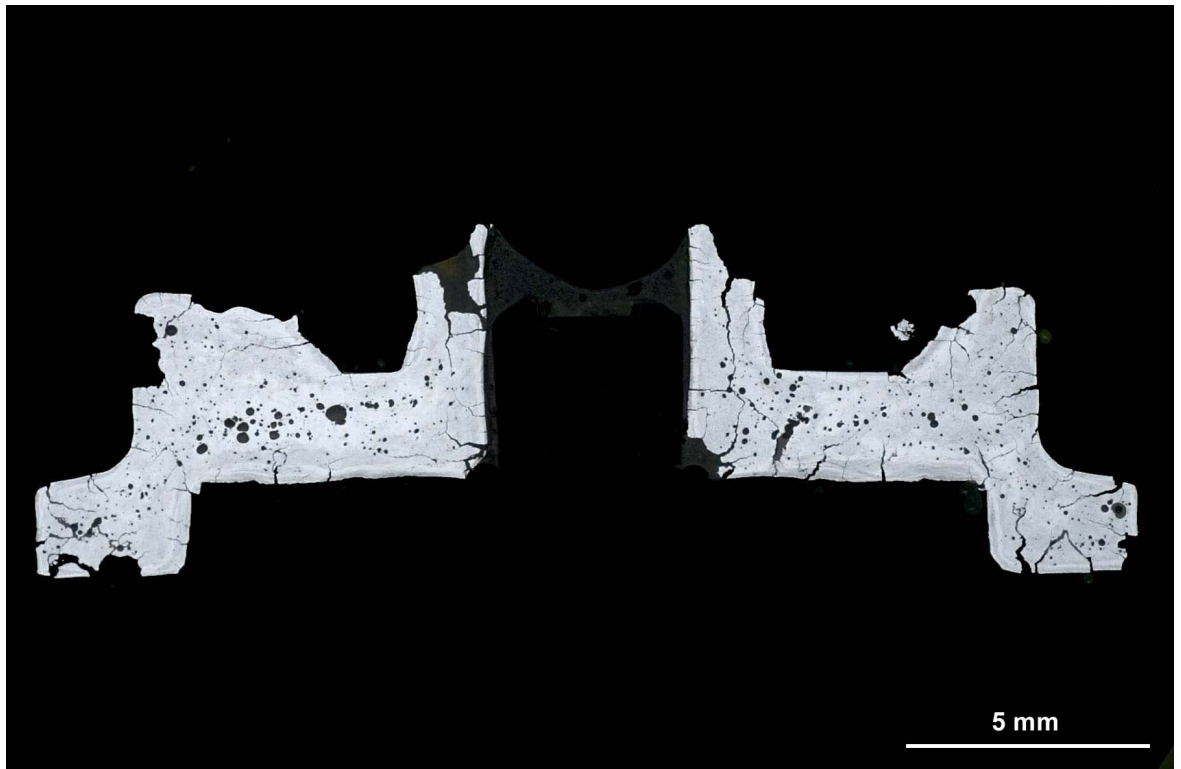


Fig. 5 Metallographic overviews of the cracking in the wheel (top) and block (bottom). Note the porosity also

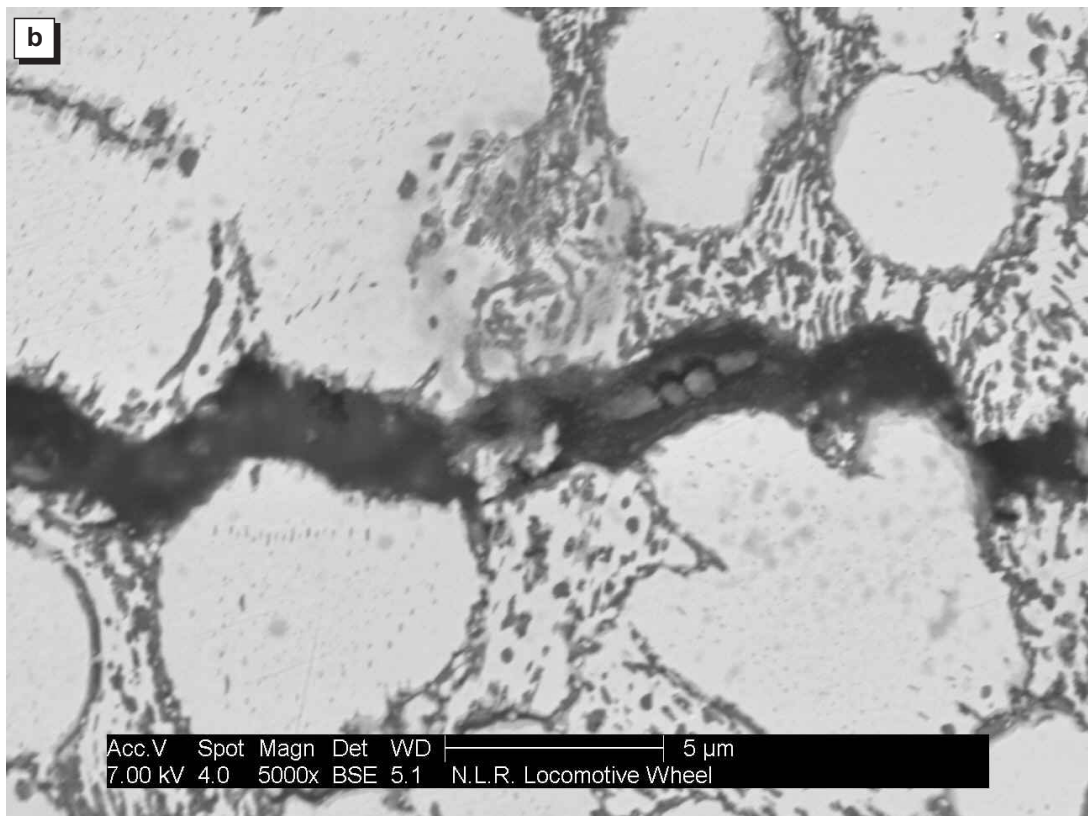
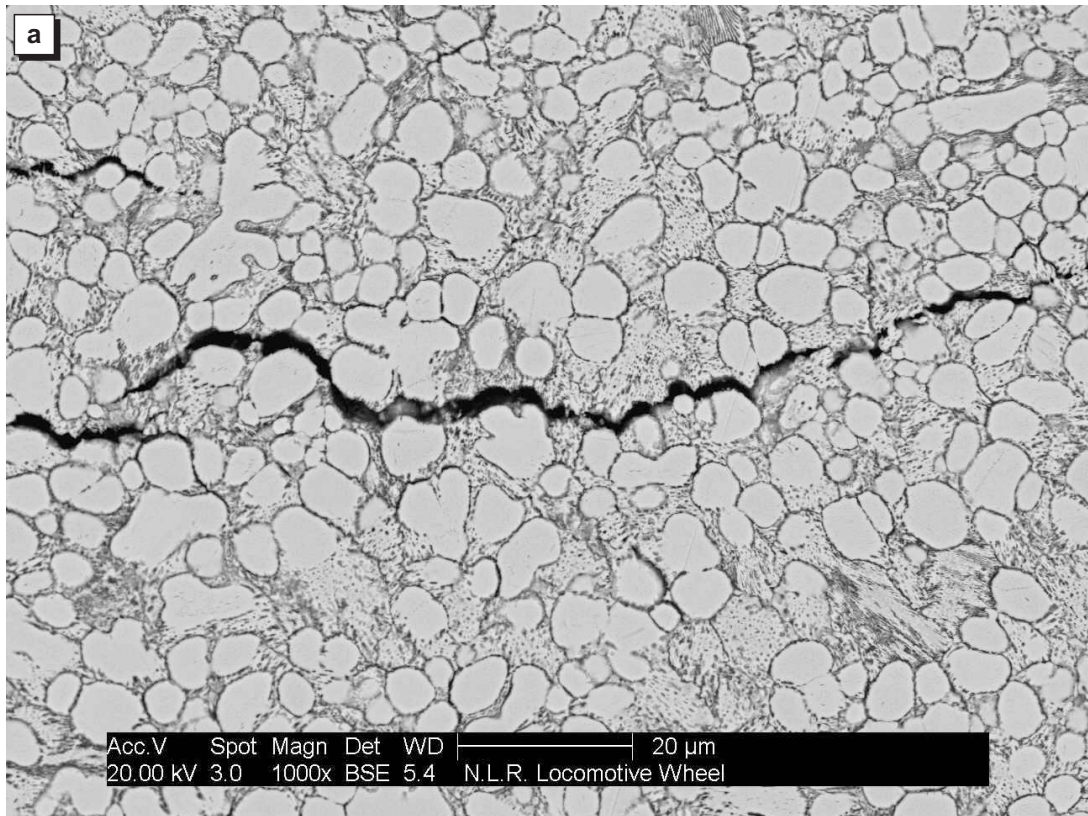


Fig. 6 Characteristics of cracking in the wheel: (a) overview of crack path predominantly along β crystal boundaries; (b) corrosion products filling the crack

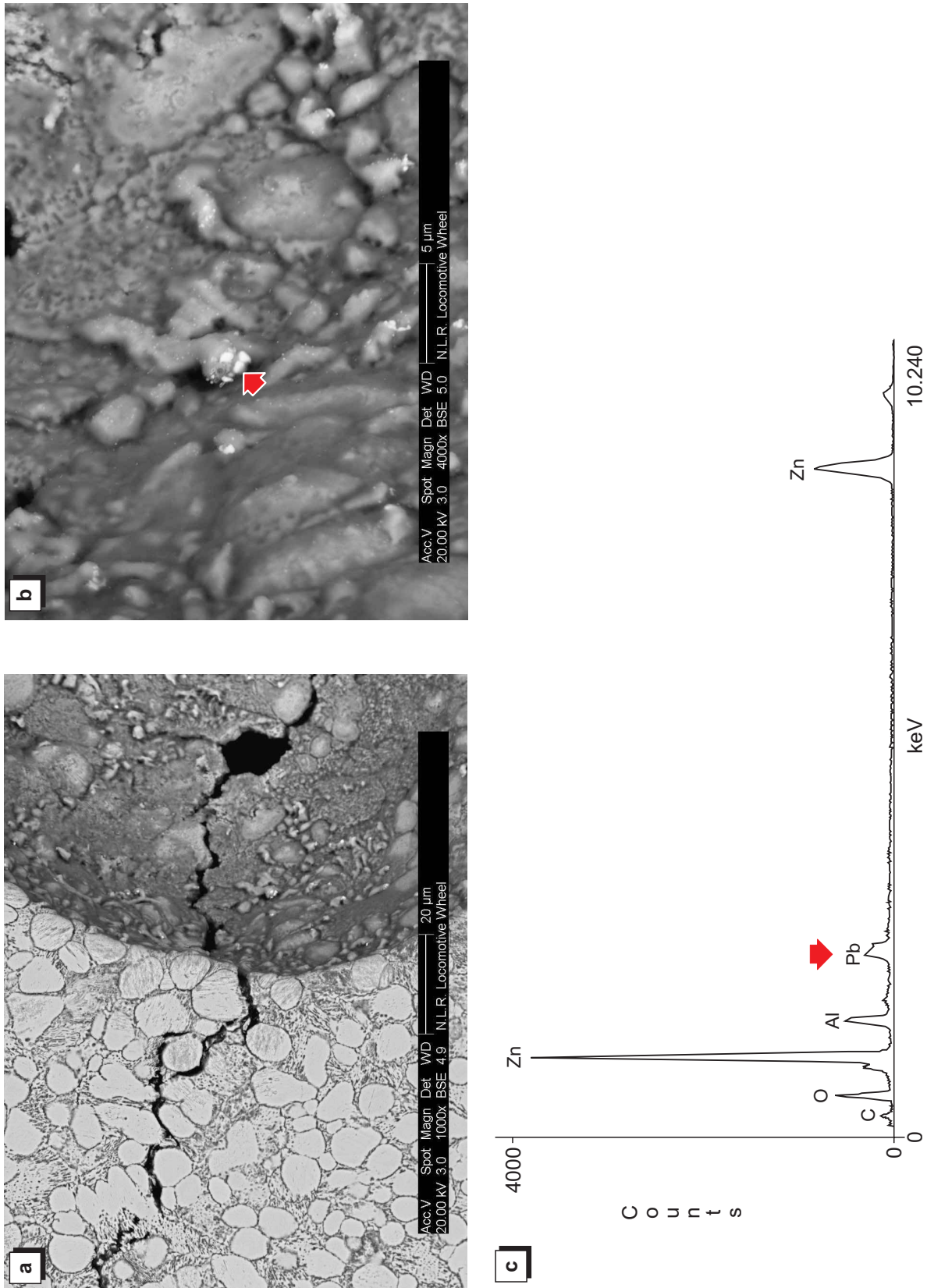


Fig. 7 Cracking in the wheel, intersecting porosity wall: (a) overview; (b) detail showing tiny particles on porosity wall; (c) EDX of the particle arrowed in (b), showing it to the lead

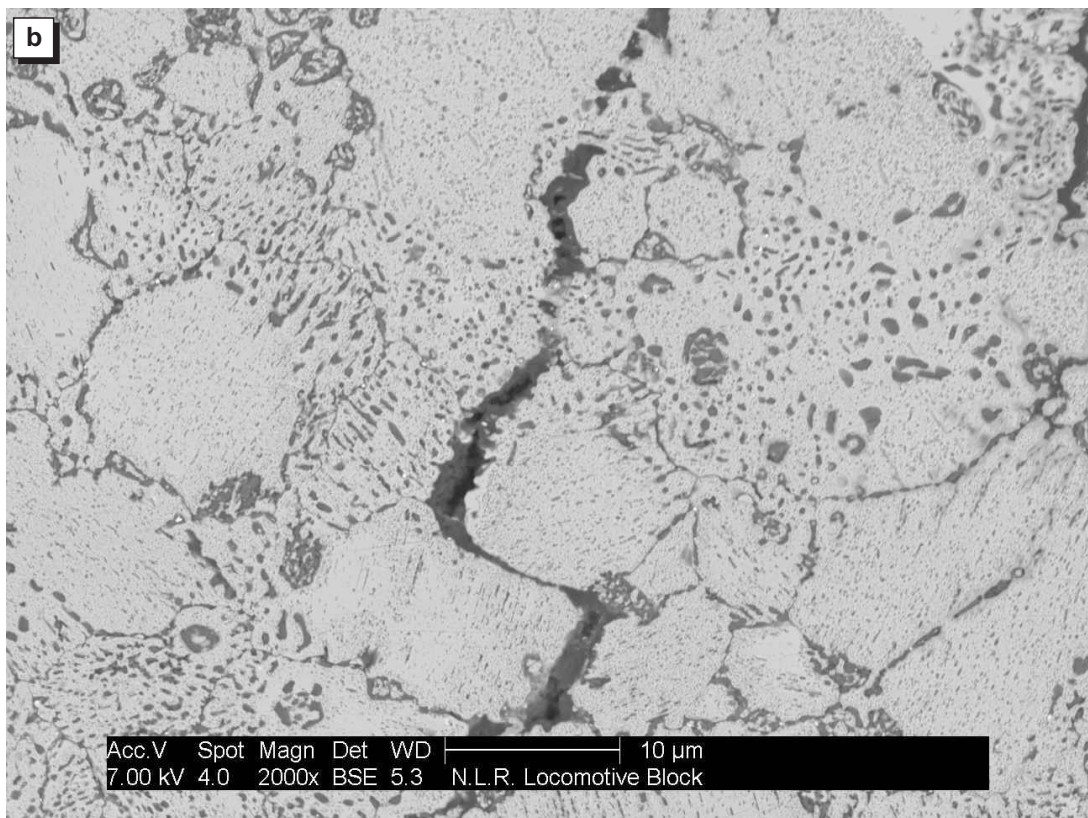
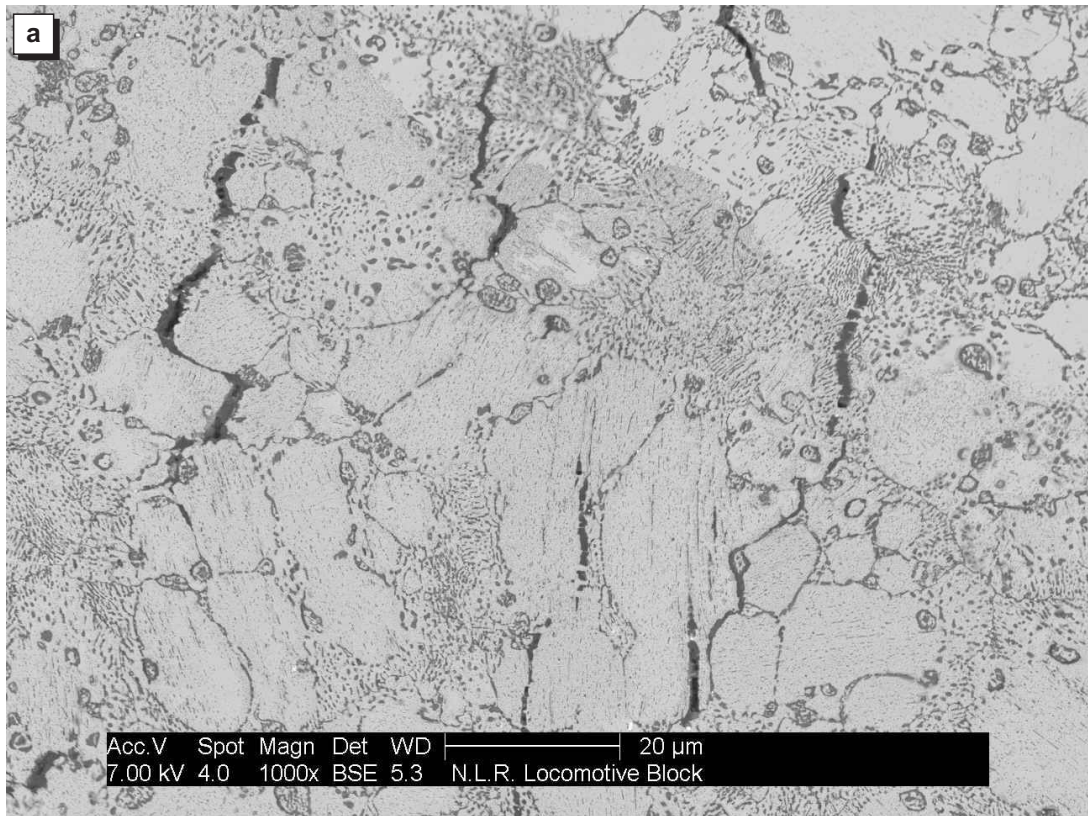


Fig. 8 Characteristics of cracking in the block: (a) overview of crack path favouring β crystal boundaries; (b) corrosion products largely filling a crack

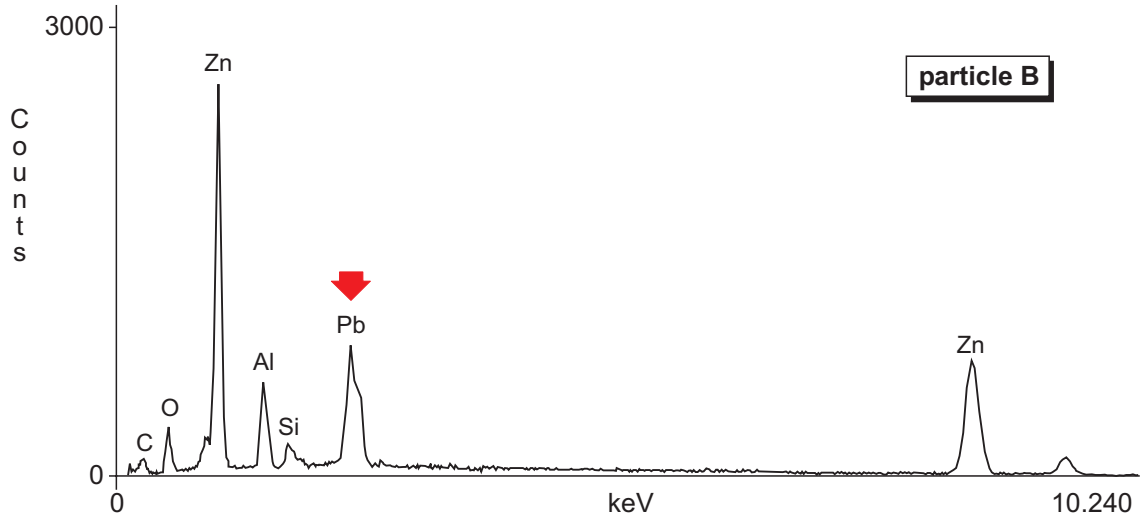
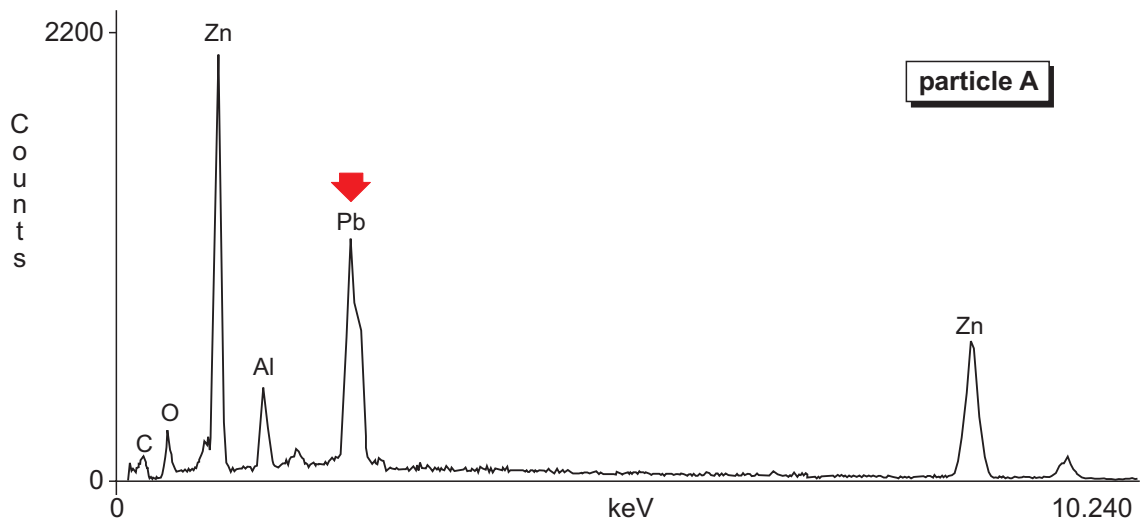
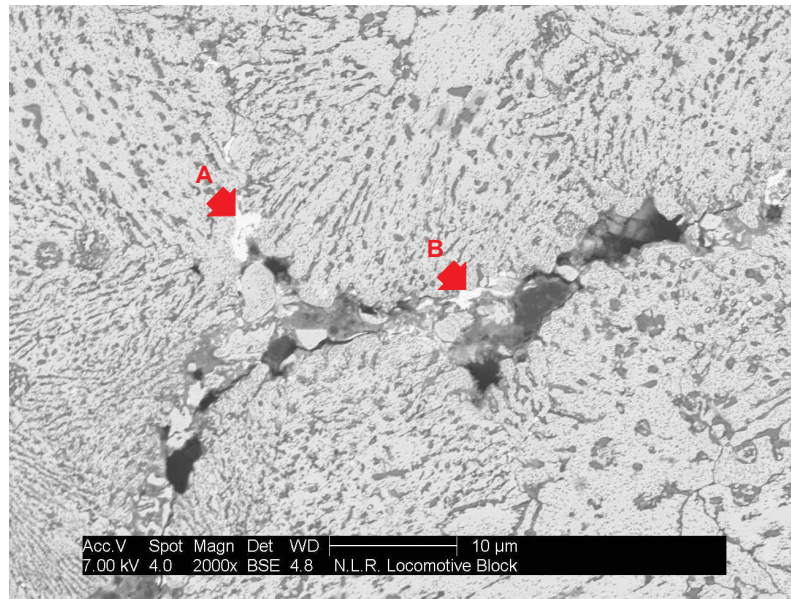


Fig. 9 Corrosion products largely filling a crack and lead particles along crack paths (two analysed by EDX)